Acoustic bubble detection - I: The detection of stable gas bodies

by Dr T G Leighton
Institute of Sound and Vibration Research,
University of Southampton,
Highfield, Southampton SO17 1BJ

The ability to detect and measure bubbles within liquids is of importance to a wide range of applications. In this paper the optical and especially the acoustic techniques appropriate to populations of stable bubbles, or gas bodies, will be examined. In a second paper, techniques appropriate to transient cavitation will be discussed. This article contains material from The Acoustic Bubble (TG Leighton), Academic Press, London, 1994.

Bubble detection is required for many industrial applications, including the preparation of molten glass or polymer solutions [**1**], and filling operations in the paint, food, detergent, cosmetics and pharmaceutical industries where bubbles may degrade the product [**2**]. In the petrochemical industry alone, bubble detection is required to optimise harvesting and transportation. Gas which had dissolved into the crude in the high pressures at the well base exsolves as the crude is brought up to surface pressures. Bubble detection in the bore may warn of high-pressure gas pockets. In hydroelectric stations, bubble detection gives warning of cavitation.

Ultrasonic probes will interact with bubbles, and can be found in the nuclear power industry [**3-7**], where passive acoustic emissions can be used for monitoring [**8**]. Ultrasonic bubble detection has other industrial applications, including fluid processing [**9**], pressure measurement [**10**], and pressure vessel monitoring [**11**]. Medical applications include studies of decompression sickness [**12,13**], and contrast echocardiography [**14**]. Bubbles *in vivo* can be detected actively [**15**] and passively [**16-19**].

Bubbles in the ocean have applications for underwater communications (eg, background noise [**20**], signal channelling [**21**], and sensing [**22**]); and monitoring of methane seeps, rainfall [Ref. **19** §3.7.2] and gas flux between ocean and atmosphere. More than 1000 million tonnes of atmospheric carbon dissolve into the seas each year [**23**]. Fluxes of carbon dioxide [**24,25**] and dimethylsulphide [**26,27**] have climatic significance [**28**].

A bubble in liquid will in general contain a mixture of permanent gas and vapour [**9,29**], and will be approximately stable over timescales where dissolution and buoyancy may be neglected if the partial pressure of the gas component roughly counterbalances the constricting pressures due to surface tension and the pressure in the surrounding liquid (which may consist of acoustic or hydrodynamic pressure perturbations superimposed upon a hydrostatic field). An acoustic field can drive it into nonlinear pulsation (termed 'stable cavitation'), which at small amplitudes approximates to the motion of a single degree of freedom linear oscillator. Shape and surface oscillations may also occur, and may be associated with microstreaming flows about the bubble. This paper discusses bubbles which, owing to the significant mass of gas contained, are approximately stable (so-called 'gas bodies'). Pt II outlines the detection of cavities which at maximum size contain insufficient gas to prevent energetic collapse ('transient cavities')

Detection techniques

These two forms of behaviour, stable and transient cavitation, can produce effects within the liquid which may be interpreted to gain information about the bubble population (Fig 1). Rapid bubble volume changes generate acoustic signals, those associated with stable gas bodies usually reflecting the characteristics of the nonlinear oscillator. Transient cavitation may generate rebound shocks, and mechanical (especially erosive) and chemical effects, the interpretation of which is sometimes less readily related to direct cavitational characteristics. Optical techniques are in contrast often readily interpreted, but are unsuitable for small bubbles, or opaque liquids or containers. Two-dimensional optical images can be difficult to relate to the volume of the bubble if it exhibits the deviations from sphericity (either oscillatory or in equilibrium shape) common in large bubbles. In contrast the pulsation resonance frequency reflects the bubble volume, and varies roughly inversely with the equilibrium radius (R_0), making it suitable for sizing small bubbles.

Therefore optical measurements have limited applicability, but are more readily interpreted than the erosive and chemical effects generally associated with high energy cavitation. The limitations arise through our understanding of mechanisms. Acoustic techniques represent a good compromise, and can be applied *in situ* to low-energy cavitation in opaque conditions.

Optical detection techniques

Optical techniques which are applied under (usually laboratory) controlled conditions include: exsolution visualisation on pressure reduction above liquids [**30**]; Mie scattering [**35-41**]; and light and electron microscopy [**31-34**] (resolv-

ing radii down to 10^{-9}m [**31,34**]). Holograms [**42**], which have resolved down to about 10μm radius [**43,44**], have been taken at up to 300,000 holograms/s [**45-47**]. Field measurements generally afford less sophisticated techniques. At sea [**48**], photography of bubbles either risen onto a transparent plate [**49**] (though they may dissolve on rising [**50**]) or *in situ* [**51**] may lack the resolution to accurately count the smallest bubbles [**52**] and poor statistics may also have limited observations [**53**].

Acoustic detection techniques

Much optical detection does not require either stable or transient bubble volume change, which is generally prerequisite for erosive and chemical detection. One acoustic technique which does not require a bubble volume change is the shadowing caused by the geometrical scattering of ultrasound having a wavelength very much smaller than the bubble radius at the bubble wall, an interface of high acoustic impedance mismatch. In this way the total surface area of bubble interface in the population as a function of position within a pipe cross-section has been tomographically mapped [**54**].

Other acoustic techniques respond either to the bubble as a stable oscillator (though in general the amplitude of oscillation required can be much smaller than necessary for detection through damage and chemical effects), and will be discussed here. The detection of a transient cavity, which briefly attains a size much greater than equilibrium, and then collapses with the emission of rebound shocks etc., will be outlined in Pt II. These techniques are not mutually exclusive, and their invasiveness should be remembered (Fig 1).

(a) Detection through 'linear' oscillations: The efficacy of these acoustic techniques for detection of 'stable' bubbles relies on three factors: (i) the ability of the bubble to act as an oscillator which approximates to linearity at small amplitude with a well-defined resonance; (ii) the excellent coupling between the sound field and the bubble, as evidenced by the high values taken by the acoustic scattering cross section at resonance; and (iii) the ability of a bubble population to impart equivalent acoustic bulk properties to a medium. These properties are employed in most experiments which exploit the oscillator properties of the bubble ((ii) and (iii) require (i) as prerequisite).

(i) The bubble as a oscillator: The natural frequency υ_0 of a spherical bubble pulsating in an inviscid liquid can be expressed as [**19** §3.4.2b]

$$\upsilon_0 = \frac{\omega_0}{2\pi} = \frac{1}{2\pi R_0}\sqrt{\frac{3\kappa p_0}{\rho}\left(1+\frac{2\sigma}{p_0 R_0}\right)-\frac{2\sigma}{\rho R_0}} \qquad (1)$$

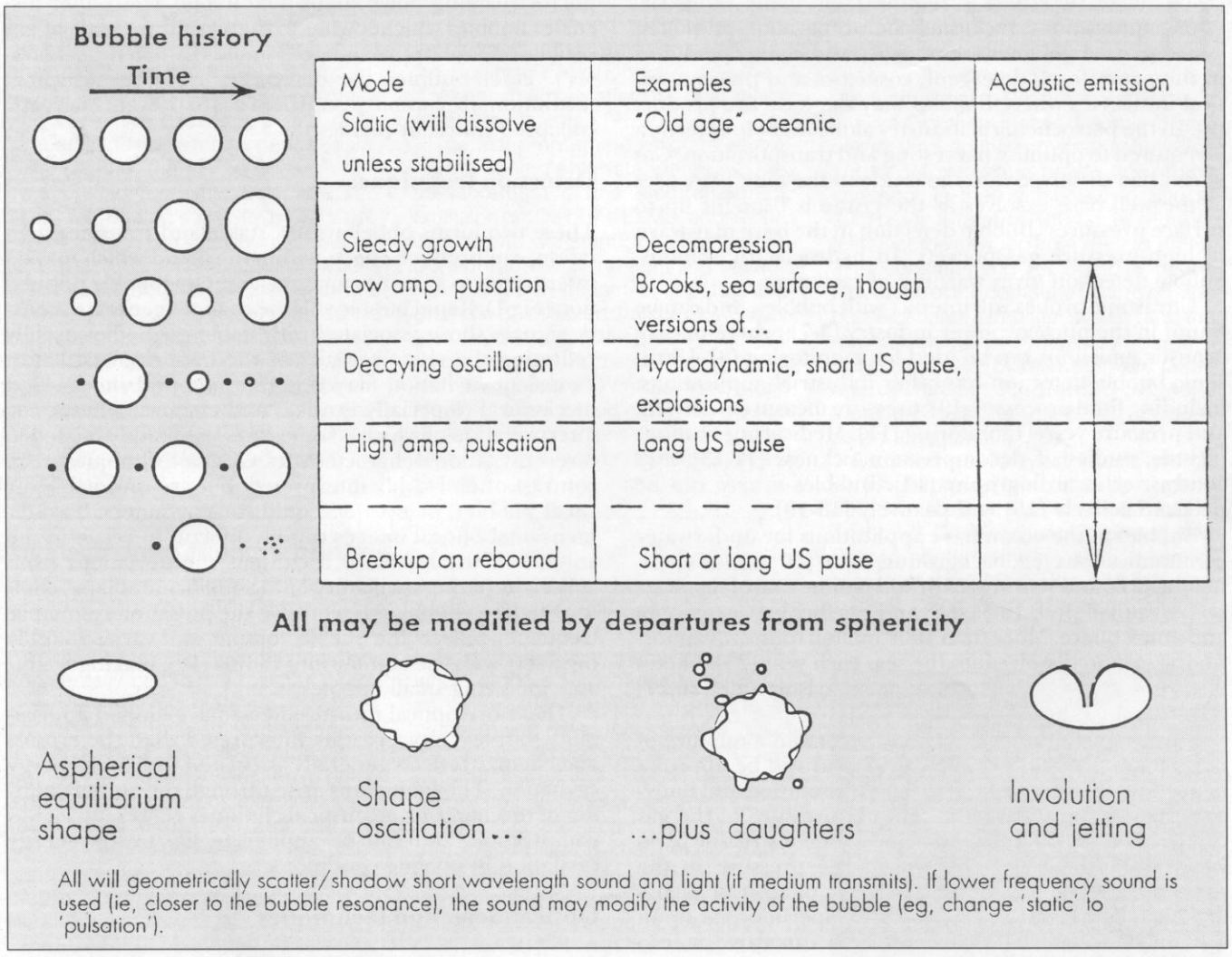

Fig 1. Some idealised bubble histories, with examples. Non-invasive acoustic detection of static bubbles or steadily growing bubbles can only be achieved through low amplitude shadowgraphy or related techniques. Stable bubbles may undergo free or forced oscillation, and generate or scatter sound appropriately. Transient cavities grow explosively, then collapse violently, emitting a rebound shock. Shape and fragmentation features may occur. After Leighton [19].

where ρ is the liquid density, σ the surface tension, and p_0 the static pressure (first derived neglecting surface tension [**55**]). The polytropic index κ varies between γ (for the adiabatic case) and unity (isothermal processes). For macroscopic air bubbles in water under one atmosphere, equation 1 reduces to [**56**]:

$$v_0 R_0 \approx 3 s^{-1} m. \qquad (2)$$

Studies on injected bubbles [**55,57-60**] showed the underwater acoustic emission to approximate to an exponentially-decaying sinusoid typical of a lightly-damped oscillator. Such bubble signatures can be used to detect and size bubbles (Fig 2) under waterfalls [**59,61**], rainfall [**62-65**], and breaking waves [**66,67**]. Since the freely oscillating bubble must first be excited in order to emit in this manner when passive emissions are used for bubble detection, the signal samples not the whole population, but only those bubbles entrained during the period of observation. The acoustic detection of older bubbles, which persist but whose entrainment emissions have ceased, requires those bubbles to be further excited to radiate or scatter sound. An example of this is the exploitation of the Doppler shift on signals from the moving bubbles in blood [**68**], which can distinguish them from reflections from static objects. However Doppler techniques may be unable to distinguish between a single large bubble and a cluster of smaller ones [**10**]. Formulation of the ability of bubbles to scatter sound is most usually done using the concept of the acoustic cross-section. In the next section, such resonance scatter is examined.

(ii) Acoustic scatter from bubbles: The acoustic scattering cross-section, Ω_b^{scat}, is defined as the ratio of the time-averaged power scattered by the bubble from a plane wave to the intensity of that plane wave. If the bubble is assumed to be a linear oscillator, it is given by

$$\Omega_b^{scat} = \frac{4\pi R_0^2}{((\omega_0/\omega)^2 - 1)^2 + (2\beta_{tot}/\omega)^2} \qquad (3)$$

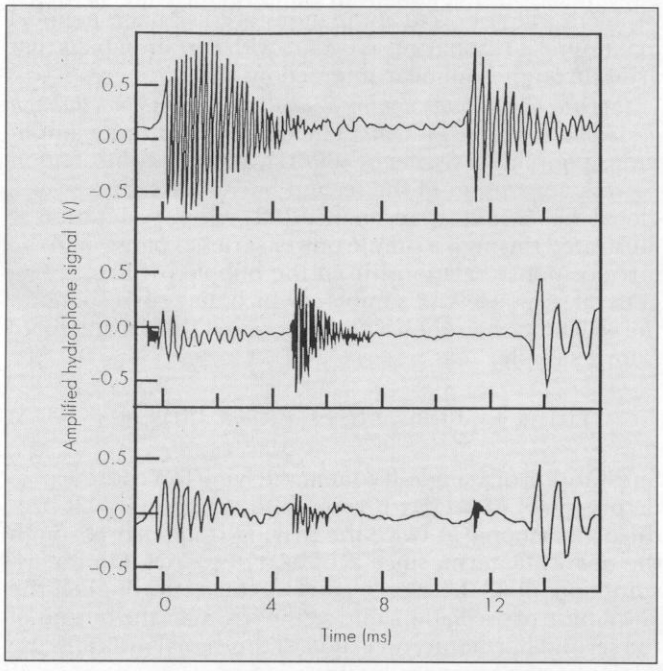

Fig 2. Sections of the hydrophone record from a babbling brook (after [59]). Each exponentially-decaying sinusoid indicates the entrainment of a bubble, and the frequency of the sinusoid gives the bubble size through equation 1.

in the limit $kR_0 << 1$, where ω_0 and $\omega = ck$ are the radian frequencies of the bubble resonance and the insonating frequency respectively, and β_{tot} is a parameter associated with the damping of the bubble [**19** §4.1.2d). For a fixed

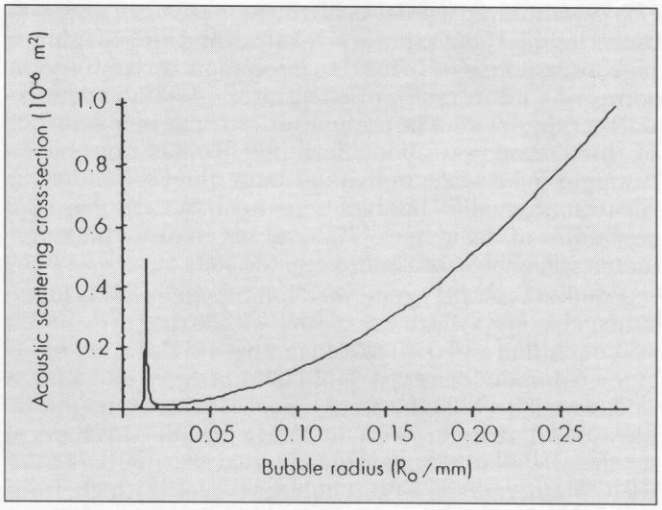

Fig 3. The scattering cross-section of a bubble, for which the damping is assumed to be constant with frequency. Linear harmonic bubble pulsations assumed. Insonation at 248kHz for quality factor Q=15. The peak at $R_0 \approx 0.013$mm indicates the pulsation resonance. After Leighton [19].

insonation frequency, this quantity is locally a sharp maximum at resonance for lightly-damped bubbles (Fig 3). Medwin [**69**] noted two facts which make the technique very suitable for bubble counting, provided that much larger scatterers are not present: Firstly, the scattering cross-section of a bubble is about 1000 times its geometrical cross-section at resonance, and about 10^{10} times that of a rigid sphere; and secondly the resonance frequency varies inversely with the radius if surface tension effects are negligible (equation 1), thereby facilitating the observation of small bubbles. However the approximation which is often employed, namely that *only* resonant bubbles scatter a given sound field, is not rigorous: There are two counter indications (Fig 3). Firstly, in conditions of finite damping, bubbles close to resonance size will contribute. Secondly, the peak at resonance is only a local minimum, such that bubbles much larger than resonance can scatter to a greater degree than those at resonance. The scattering by resonant bubbles is due to the strong coupling with the incident wave, as manifested by the large amplitude of wall pulsation. Much larger bubbles in contrast pulsate to a negligible degree: in the limit of the bubble size being much larger than the acoustic wavelength, the process is geometric, the bubbles generating acoustic shadows. It should be remembered that the formulation of equation 3 is for the linear limit: in many cases where acoustic techniques are deployed in this manner, in order to generate a sufficiently high signal-to-noise ratio the sound field is strong enough to impart a degree of nonlinearity into the bubble oscillation.

Studies which have exploited the enhanced scattering from resonant bubbles include both oceanic sonar studies [**70,71**] employing frequencies up to about 200kHz, and medical studies involving ultrasound of higher frequency. Decompression bubbles have been imaged [**72**]; the returning echo strength at 7.5MHz *in vivo* in humans, fish, and guinea pigs has been taken to be a measure of the bubble size (calibrated through comparison of microscopic and ultrasonic measurements on bubbles in water, gelatin,

and transparent fish) [**73**]. However small bubbles close together scattered incoherently such that they could not be distinguished from single, larger bubbles.

By the early 1980's there was evidence of ultrasonically-generated cavitation effects *in vivo* [**74-76**]. ter Haar et al. [**77-79**] employed a pulse-echo ultrasonic B-scan system to detect bubbles generated *in vivo* in the hind limbs of guinea pigs in response to 0.75MHz insonation by continuous-wave or 1 : 1 duty cycle pulsed ultrasound from a commercial therapy device. The minimum detectable bubble radius of this system was about 5μm [**80**]. It was not able to distinguish between individual large bubbles and tight clusters of smaller bubbles separated by less than the resolution of the system [**77**], and no accurate measurements of bubble size could be made [**80**].

Fowlkes et al. [**81**] generated bubbles in excised canine urinary bladders which were sealed within a bag of degassed saline solution and then placed in a bath of degassed water at the common focus of a 555kHz transducer and a brass reflector. The bubbles were visualised on a diagnostic ultrasound scanner with a 5MHz in-line mechanical scanhead. Pressure amplitudes as great as 10-20 bars were used to generate the largest bubbles detected which, from their rise times, had estimated radii of 50-70μm. These bubbles, being very much larger than resonance, were probably generated through coalescence in the standing-wave field in the bladder. As regards detection of the smaller bubbles, the inability to distinguish bubble echo from artefacts caused by the reverberant field within the bladder set resolution limits.

Bleeker et al. [**82**] used the attenuation coefficient, sound speed and backscatter coefficients at 5 and 7.5MHz to examine a controlled population of Albunex* spheres, a commercial echo-contrast agent for clinical applications, which consists of microbubbles in the size range $0.5\mu m<R_0<5\mu m$ stabilised against dissolution by a shell approximately 28nm thick made of coagulated human serum albumin.

Exploitation of the resonance featured explicitly in the 1977 study of Fairbank and Scully [**83**], who examined the emitted scattered signal from bubbles, assumed to be at resonance, subjected to broad band ultrasound (from 100kHz to 1MHz). They proposed using this technique in order to measure blood pressure changes in inaccessible regions of the heart through the resulting changes in the equilibrium volumes of injected bubbles. However resonance techniques are not ideal. Simulations of common methods of bubble sizing through resonance techniques for hypothetical bubble size distributions by Commander and Moritz [**84**] suggests that the number of bubbles having $R_0<50\mu m$ can be significantly overestimated. More thorough analyses of data are required to compensate (see, for example, Commander et al. [**85**]).

(iii) Equivalent bulk properties: Techniques which exploit the ability of a bubble population to impart equivalent bulk properties to a volume of the medium through which it is evenly distributed are generally interpreted through an analysis which suffers the same inherent limitations as the above technique, in that linear theory is employed in the interpretation, and in that it is assumed that only resonant bubbles contribute. However, they enable measurements to be made in the limit of high population densities, where most other techniques are inapplicable. An example of such a bulk parameter is the sound speed, which for longitudinal waves in a continuum depends on the square root of the ratio of bulk modulus and the density. The addition of bubbles to a liquid reduces the bulk modulus (or, equivalently, increases the compressibility) of the resulting mixture when it in turn is viewed as a continuum, to a far greater extent than it reduces the density. Therefore the sound speed falls to less than that of the bubble-free liquid (c), and in a sufficiently bubbly mixture can be less than that of the gas phase alone (owing to the contribution of the liquid phase to the density). If there is a distribution of bubble sizes within the cloud, such that $n^{gr}(z,R_0)dR_0$ is the number of bubbles per unit volume at depth z having radii between R_0 and R_0+dR_0, the speed of sound c_c is a function of both the depth and the acoustic frequency:

$$c_c(z,\omega)=c\{1-(2\pi c^2)\int_{R_0=0}^{\infty}\frac{R_0}{\omega^2}\left(\frac{(\omega_0/\omega)^2-1}{\{(\omega_0/\omega)^2-1\}^2+d^2}\right)n^{gr}(z,R_0)dR_0\}, \quad (4)$$

where d is a dimensionless damping parameter [**19** §4.1.2e; **86**]. An example of an acoustic device which exploits such bulk properties is the simple resonator of Medwin and Breitz [**87,88**]: the resonance frequencies of the device when it is filled with bubbly liquid are less than those when it is bubble-free as a result of the reduced sound speed; similarly the widths of the resonances are broadened since the bubbles introduce greater dissipation. Such dissipation increases attenuation, which has been used to monitor ocean bubble population *in situ* [**69**]. The study included measurements of scattering and phase velocity, though dispersion was too small to measure accurately.

To insonate a sample of bubbly liquid at a frequency ω, and assume that variations in the signal at ω are caused by bubbles resonant with the frequency ω, is to assume that the ω signal is yielding information about resonant bubbles only. However the resonance peak is only a local, and not a global, maximum (Fig. 3): The signal at ω may be affected by other than resonant bubbles, and interpretation in terms of resonant bubbles only may be incorrect. This problem will not occur if the monitored signal is a global maximum at resonance, as occurs with certain signals that arise through nonlinear interactions.

(*b*) *Detection through nonlinear oscillations: Detection through the second harmonic emission:* The bubble is, at finite amplitude, a nonlinear oscillator [**89-91**], and at low insonation powers generation of the second harmonic signal gives a global maximum at resonance [**92**]. This generation is illustrated through a simple power series expansion of the force/response relationship in the bubble oscillator. The general response Y of a bubble (which may correspond to the wall motion) is then a power series of the driving force f, for example,

$$Y(t)=s_0+s_1.f(t)+s_2.f^2(t)+s_3.f^3(t)+s_4.f^4(t)+\ldots, \quad (4)$$

Substitution of a single-frequency driving force (the acoustic pressure) of $f\equiv P(t)=P_A\cos\omega t$ into equation 4 will produce a harmonic at twice the driving frequency through the quadratic term, since $2\cos^2\omega t=1+\cos 2\omega t$. On the assumption that, the closer to resonance, the higher the amplitude of oscillation, and so the stronger the output of the second harmonic, detection of this signal indicates the presence of a resonant bubble.

The "resonant bubble detector" (RBD) [**93**] used two transducers, a 1.64MHz emitter (0.12W cm^{-2}) and a 3.28MHz receiver, mounted with suitable acoustic ab-

* Albunex is a trade mark of Molecular Biosystems Inc, 10030, Barnes Canyon Road, San Diego, California, USA.

sorber, their axes perpendicular to each other and to the 4mm diameter tube containing the flowing liquid that was to be investigated. The detector, tuned to twice the emitter frequency, was sensitive to bubbles sizes resonant with the emitter ($R_0 \approx 2.1\mu m$ for 1.64MHz). Miller et al. [**94**] used a larger, modified detector such that the interrogated region was 7.4mm from each transducer, with the emitter operating at 0.89 or 1.7MHz. Miller [**93**] tested the device for two bubble sizes in water: the second harmonic emitted by resonant bubbles (produced by electrolysis) was 43 times stronger than that produced by injected bubbles of 250μm radius. By comparison the fundamental emission from the resonant bubbles was 0.02 times that from the larger bubbles.

Miller et al. [**94**] were able to semi-quantitatively detect bubbles produced by upstream ultrasonic cavitation, and by hydrodynamic cavitation at a detector tip, though they speculate that coalescence and radiation forces may have affected the population, and the detector responded to some bubbles which were up to 25% larger or smaller than resonance. In 1985 Gross et al. [**18**] were unable to detect bubbles downstream from the aorta when canine hearts were and were not insonated. In 1984 Vacher et al. [**95**] produced a similar bubble detector, though the frequency of interrogation (and therefore the size of bubble that was resonant) could be swept, the detector frequency being constantly twice that of the emitter. Spatial resolution is poor with the second harmonic technique [**10**]. Another drawback is that the second harmonic may arise through nonlinear effects when sound propagates through even bubble-free water [**96,97**].

Detection through combination frequencies: The power series model of the bubble as a nonlinear oscillator (equation 4) can be used to illustrate how the use of two insonating frequencies can detect and size bubbles. If the driving force consists of the sum of two coherent forces of different frequency, ie.

$$f \equiv P(t) = P_1 \cos\omega_1 t + P_2 \cos\omega_2 t, \quad (5)$$

where $\omega_2 > \omega_1$ (the presence of phase constants would not alter the general result) the quadratic component contains a term which can be expanded to generate the sum and difference frequencies:

$$2P_2P_1 \cos\omega_1 t \cos\omega_2 t = P_2P_1\{\cos(\omega_1+\omega_2)t + \cos(\omega_2-\omega_1)t\} \quad (6)$$

Newhouse and Shankar [**98**] describe the sizing process using the scattered signals generated when a bubble is insonated with a 'pump' frequency ω_p and an 'imaging' frequency ω_i. Experimentally, Shankar et al. [**10**] used a 2.25MHz 'imaging' beam, the pump signal being scanned across the frequency domain where the bubble resonance could reasonably be expected to lie. When the pump frequency is far from the bubble resonance, the bubble response is of small amplitude and it approximates to a linear oscillator. In that situation, therefore, no sum- and difference-frequencies are detected. When ω_p is near the bubble resonance, the amplitude of oscillation of the bubble wall is large. The bubble oscillations are nonlinear, and they scatter sound nonlinearly. As with the second harmonic, these combination frequencies exhibit a global maximum at resonance, and Shankar et al. [**10**] therefore took the frequency of the pump signal when the sum- and difference-frequencies ($\omega_i \pm \omega_p$) are detected to be the bubble resonance, and so had a measure of the bubble size. Geometrical screening of smaller bubbles by larger ones may occur [**99**]. Clinical echocontrast bubbles [**100, 101**] and cylindrical gas pockets trapped in hydrophobic pores [**102-105**] of μm size have been sized. The fractional Doppler shift, f_{Dop}, in the received signal (the detected frequencies including ω_i, $\omega_i \pm \omega_p$, $(1+f_{Dop})\omega_i$, and $(1+f_{Dop})\omega_i \pm \omega_p$) can give bubbles size, direction, number density and speed information [**106**], and ranges when pulsed [**107**], giving lateral and longitudinal resolution of better than 1mm. Bubbles acting in structured populations may give rise to combination frequencies [**90,108**].

The nonlinear oscillations of strongly-driven bubbles can give rise to subharmonic emissions (Fig 4). Though the power series expansion given in equation 4 will not predict subharmonics, an expansion based on Fourier series expansion or perturbation methods will do so [**109**]. These too can combine with an imaging frequency when a bubble is insonated at ω_i and ω_p,, the detected signals including frequencies at $\omega_i \pm \omega_p/2$ in addition to ω_i, ω_p,$\omega_i \pm \omega_p$, and higher-order signals [**110,111**]. The highly nonlinear nature of the subharmonic emission suggested that, if excited, it would be a very sensitive indicator of the bubble resonance, and this was confirmed by analysis and comparison of the

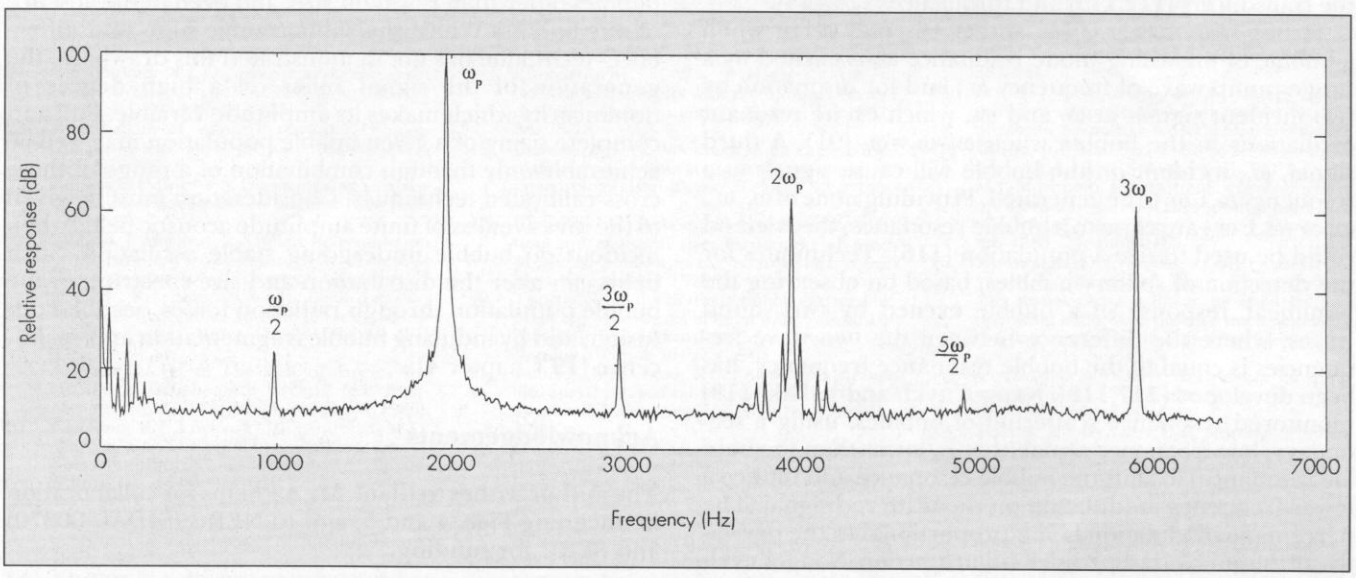

Fig 4. The spectrum of the acoustic scattered waves from a bubble insonated at resonance ($\omega_p/2\pi$=2kHz). Harmonics ($2\omega_p$, $3\omega_p$), a subharmonic ($\omega_p/2$), and ultraharmonics ($3\omega_p/2$, $5\omega_p 2$) are shown.

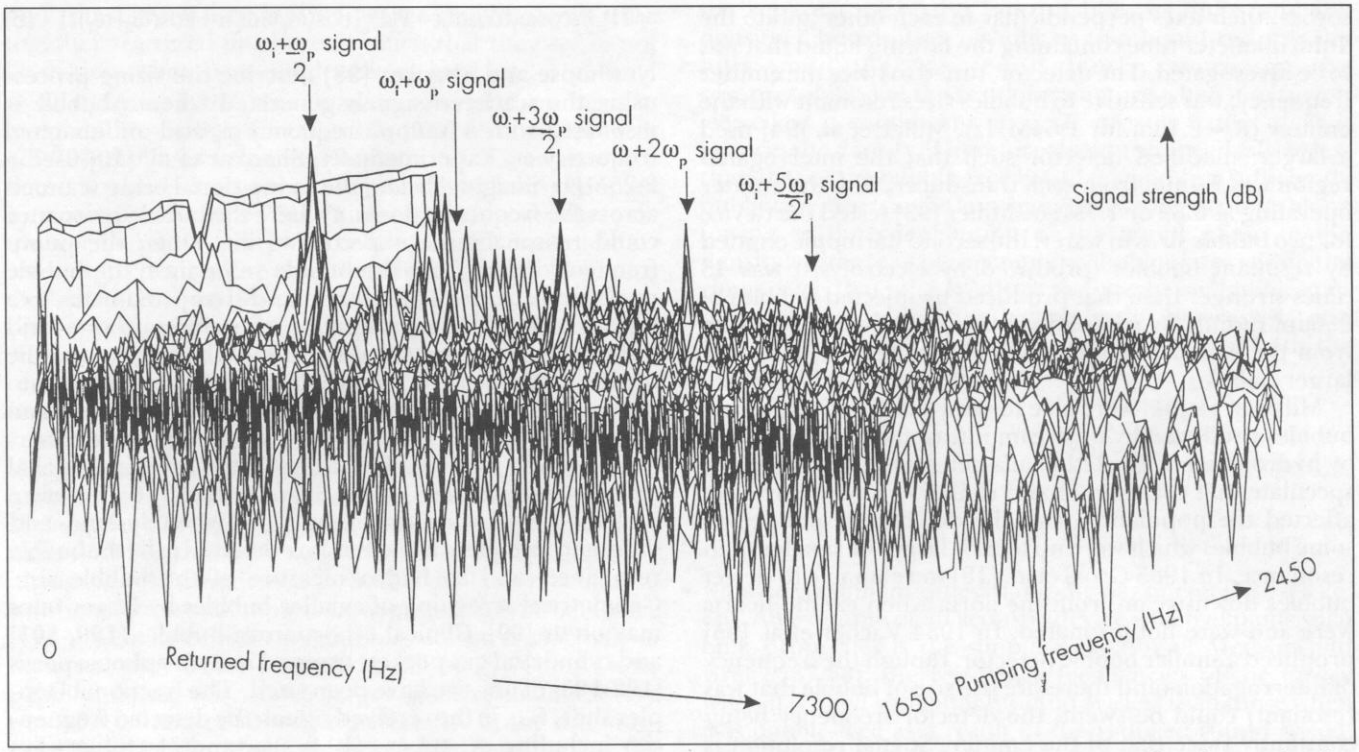

Fig 5. A mesh plot resulting from insonation of a single bubble (ω_i=1.1MHz; pump signal amplitude=58Pa zero-to-peak). The axes therefore correspond to the pump frequency setting, and the positive difference in Hz between the spectral components of the returned signal and the imaging frequency. Signals at $\omega_i+\omega_p$, $\omega_i+\omega_p/2$, $\omega_i+3\omega_p/2$, $\omega_i+2\omega_p$ and $\omega_i+5\omega_p/2$ are detected above the noise.

emissions at the various frequencies. Fig. 5 shows a mesh plot resulting from insonation of a bubble with an imaging frequency of 1.1MHz and a pump frequency of amplitude 58Pa. The pump signal is incremented in 25Hz steps, and for each setting the high-frequency emissions from the bubble are noted: the axes therefore correspond to the pump frequency setting, and the positive difference in Hz between the returned spectral components and the imaging frequency. The bubble resonance (2125Hz) is clearly indicated by the signals at $\omega_i+\omega_p/2$, $\omega_i+3\omega_p/2$, $\omega_i+2\omega_p$ and $\omega_i+5\omega_p/2$: however, the $\omega_i+\omega_p$ signal contains significant off-resonance components. The $\omega_i+\omega_p/2$ signal may be a better sizing tool than $\omega_i+\omega_p$, as it is sharper and cannot readily be excited through non-bubble mechanisms, such as direct coupling of the transducers [**112,113**] and turbulence [**114,115**].

Strong response at $\omega_1-\omega_0$ and $\omega_1+\omega_0$ may occur when a bubble of breathing-mode resonance ω_0 is excited by a single pump wave of frequency ω_1; and for insonation by two incident signals at ω_1 and ω_2, which excite resonant oscillations in the bubble when $\omega_1-\omega_2=\omega_0$ [91]. A third signal, ω_3, incident on the bubble will cause signals at a frequency $\omega_3\pm\omega_0$ to be generated. Providing none of ω_1, ω_2, ω_3 or $(\omega_3\pm\omega_0)$ are close to a bubble resonance, this method could be used to size a population [**116**]. Techniques for the detection of solitary bubbles, based on observing the nonlinear response of a bubble excited by two sound waves, where the difference between the two wave frequencies is equal to the bubble resonance frequency, has been developed [**117,118**]. Naugol'nykh and Rybak [**119**] monitored resonance scattering of bubbles, using a secondary, low-frequency signal (that is, lower than the bubble resonance) to shift the bubble resonance and induce a lower-frequency modulation on the scattered signal. The percentage modulation being proportional to the derivative of the bubble-radius distribution function, Naugol'nykh and Rybak predict that the distribution could be reconstructed from the scattered signal.

Conclusions

There are a variety of methods that may be employed for the detection of stable bubbles. Whilst optical techniques can readily be interpreted (to give, for example, bubble shape) they are difficult to use in opaque environments and most give two-dimensional images. Apart from shadowgraphy, the acoustic techniques described all fundamentally rely on exploiting the bubble as a resonator. Whilst passive emissions can be used to determine the population upon entrainment, other techniques are required to examine the bubbles at a later time. All have advantages and disadvantages, particularly as regards the possibilities of the desired signal being extractable from bubbles other than resonant size, and even in the absence of any bubbles.Whilst the subharmonic sum- and difference- technique has not demonstrated this drawback, the generation of the signal relies on a high degree of nonlinearity which makes its amplitude variable. Full and complete sizing of a given bubble population may well be achievable only through combination of a range of these cross-calibrated techniques. Consideration must be given to the invasiveness of finite amplitude acoustic fields when incident on bubble undergoing stable oscillation. Such fields can alter the distribution and size spectrum of the bubble population through radiation forces, rectified diffusion, and by inducing bubble fragmentation and coalescence [**19** Chapter 4].

Acknowledgements

The author wishes to thank Mr A Phelps for collaboration in obtaining Figs. 4 and 5, and to NERC (SIDAL 00670) and SERC for funding.

Continued on next page

References

1. Detsch, R M, Sharma, R N, The critical angle for gas bubble entrainment by plunging liquid jets. The Chemical Engineering Journal 1990; 44: 157-166.
2. Lin, T J, Donnelly, H G, Gas bubble entrainment by plunging laminar liquid jets. AIChE J. 1966; 12: 563-571.
3. Watkins, R D, Barrett, L M, McKnight, J A, Ultrasonic waveguide for use in the sodium coolant of fast reactors. Nucl Energy, 1988; 27: 85-89.
4. Lions N et al. Special instrumentation for Phenix. Fast Reactor power stations. Thomas Telford, London, 1984, pp. 525-535.
5. Day C K, Smith R W. Undersodium viewing. IEEE Trans 1974; SU-21, No. 3, July.
6. McKnight J A et al. The use of ultrasonics for visualising components of the prototype fast reactor whilst immersed in sodium. Ultrasonics International 83. Butterworth Scientific 1983, pp 135-140.
7. McKnight J A et al. Recent advances in the technology of undersodium inspection in LMFBRs. Liquid metal engineering and technology. BNES, London, 1984; 1: 423-430.
8. Aguilar A, Por G. Monitoring Temperature reactivity coefficient by noise methods in a NPP at full power. Ann nucl Energy 1987; 14, 521-526.
9. Apfel, R E, Methods in Experimental Physics Vol. 19 (ED Edmonds, P D) Academic Press, New York 1981; 355-413.
10. Shankar, P M, Chapelon, J Y and Newhouse, V L Fluid pressure measurement using bubbles insonified by two frequencies. Ultrasonics, 1986; 24: 333-336.
11. Hulshof, H J M, Schurink, F. Continuous ultrasonic waves to detect steam bubbles in water under high pressure. Kema Scientific and Technical Reports, 1985; 3: 61-69.
12. Belcher, E O. (1980) "Quantification of bubbles formed in animals and man during decompression", IEEE Trans. Biomed. Eng., 27, 330-338.
13. Kisman, H. Spectral analysis of Doppler ultrasonic decompression data. Ultrasonics , 1977; 15: 105-110.
14 Tickner, E G. Precision microbubbles for right side intercardiac pressure and flow measurements. In: Contrast Echocardiography, Meltzer, R S, Roeland, J (eds), (Nijhoff, London). 1982.
15. Gross, D R, Miller, D L, Williams A R. A search for ultrasonic cavitation within the cardiovascular system. Ultrasound Med Biol 1985; 11: 85-98.
16. Dowson D, Unsworth A, Wright V. Proc. Tribology Conv. (London: Inst. Mech. Eng.) 1971; pp. 120-127.
17. Dowson D, Unsworth A, Wright V. Ann Rheumatic Dis 1971; 30: 348-358.
18. Dowson D, Unsworth A, Wright V. Cracking of human joints - cavitation in metacarpio-phalangeal joint. Ind Lub Tri 1971; 26: 212.
19. Leighton T G. The Acoustic Bubble. Academic Press, London, 1994.
20. Urick R J. Principles of underwater sound, 3rd edn McGraw-Hill, New York 1983; pp. 202-209.
21. Buckingham M J. On acoustic transmission in ocean-surface waveguides. Phil. Trans. R. Soc. Lond. A 1991; 335: 513-555.
22. Buckingham M. Acoustic daylight: Imaging the ocean with ambient noise. Nature 1992; 356: 327-329.
23. Anderson I, Bowler S. Oceans spring surprise on climate modellers. New Scientist 1990; 125: 1707.
24. Etcheto, J, Merlivat, L. Satellite determination of the carbon dioxide exchange coefficient at the ocean-atmosphere interface: a first step. J geophys. Res 1988; 93 (C12): 15669-15678.
25. Woolf, D K. Bubbles and the air-sea transfer velocity of gases. Atmos.-Ocean 1993; 31: 451-474.
26. Andreae, M O., in The Role of Air-Sea Exchange in Geochemical Cycling (ed. Buat-Menard, P.) 331-363 (Reidel, Dordrecht, 1986).
27. Charlson, R J, Lovelock, J E, Andreae, M O, Warren, S G. Oceanic Phytoplankton, atmospheric sulphur, cloud albedo and climate. Nature 1987; 326: 655-661.
28. Watson A J, Upstill-Goddard R C, Liss, P S. Air-sea gas exchange in rough and stormy seas measured by a dual-tracer technique. Nature 1991; 349: 145.
29. Neppiras, E A. Acoustic cavitation. Phys Rep 1980; 61: 159-251.
30. Finkelstein, Y, Tamir A. Formation of gas bubbles in supersaturated solutions of gases in water. AIChE J, 1985; 31: 1409.
31. Yount, D E, Strauss R H. Bubble formation in gelatine: a model for decompression sickness. J Appl Phys 1976; 47: 5081-5088.
32. Yount, D E, Yeung C M. Bubble formation in supersaturated gelatine: A further investigation of gas cavitation nuclei. J Acoust Soc AM 1981; 69: 702-15.
33. Yount, D E, Gillary, E W, Hoffman, D C. A microscopic investigation of bubble formation nuclei. J Acoust Soc Am 1984; 76: 1511-1521.
34. Yount, D E. Skins of varying permeability: a stabilisation mechanism for gas cavitation nuclei. J Acoust Soc Am 1979; 65: 1429-39.
35. Marston, P L. Critical angle scattering by a bubble: physical-optics approximation and observations. J. Opt. Soc. Am. 1979; Vol. 69, No. 9: 1205
36. Marston, P L, Kingsbury, D L. Scattering by a bubble in water near the critical angle: interference effects. J. Opt. Soc. Am. 1981; Vol. 71, No. 2: 358.
37. Marston, P L, Langley, D S, Kingsbury, D L. Light scattering by bubbles in liquids: Mie theory, physical-optics approximations, and experiments. Applied Scientific Research 1982; 38: 373-383.
38. Langley, D S, Marston, P L. Scattering of laser light from bubbles in water at angles from 68 to 85 degrees. SPIE 1984; Vol. 489 Ocean Optics VII: 142.
39. Langley, D S, Marston, P L. Critical-angle scattering of laser light from bubbles in water: measurements, models, and application to sizing of bubbles. Applied Optics 1984; Vol. 23, No. 7: 1044.
40. Gaitan, D F, Crum L A. Observation of sonoluminescence from a single cavitation bubble in a water/glycerine mixture. In: Frontiers of Nonlinear Acoustics, 12th ISNA. Hamilton M F, Blackstock D T, eds. (Elsevier, New York) 1990, p. 459.
41. Gaitan, D F, Crum, L A, Church, C C, Roy, R A. An experimental investigation of acoustic cavitation and sonoluminescence from a single bubble. J Acoust Soc Am 1992; 91: 3166-3183.
42. Hentschel W, Zarschizsky H, Lauterborn W. Recording and automatical analysis of pulsed off-axis holograms for determination of cavitation nuclei size spectra. Optics Communications 1985; 53: 69-73.
43. Hüttmann, G, Lauterborn, W, Schmitz, E, Tanger, H. Holography with a frequency doubled Nd:YAG laser. SPIE (Holography techniques and applications) 1988; 1026: 14-21.
44. Nyga, R, Schmitz, E, Lauterborn, W. In-line holography with a frequency doubled Nd:YAG laser for particle size analysis. Applied Optics 1990; 29: 3365-3368.
45. Hentschel, W, Lauterborn, W. High speed holographic movie camera. Optical Engineering 1985; 24: 687-691.
46. Lauterborn, W, Koch, A. Holographic observation of period-doubled and chaotic bubble oscillations in acoustic cavitation. Phys. Rv. 1987; A35: 1974-1976.
47. Hentschel, W, Merboldt, K-D, Ebeling, K-J, Lauterborn, W. High speed holocinematography with the multiply cavity-dumped argon-ion laser. J Photogr Sci 1982; 30: 75-78.
48. Blanchard, D C, Woodcock, A H. Bubble formation and modification in the sea and its meteorological significance. Tellus 1957; 9: 145-158.
49. Kolovayev, P A. Investigation of the concentration and statistical size distribution of wind produced bubbles in the near-surface ocean layer. Oceanology 1976; 15: 659-661.
50. Thorpe, S. On the clouds of bubbles formed by breaking wind-waves in deep water, and their role in air-sea gas transfer. Philos. Trans. R Soc London 1982; A 304: 155-210.
51. Johnson, B D, Cooke, R C. Bubble populations and spectra in coastal waters: a photographic approach. J. Geophys. Res. 1979; 84, C7: 3761-3766.
52. Walsh, A L, Mulhearn, P J. Photographic measurements of bubble populations from breaking waves at sea. J Geophys Res 1987; 92: 14553-14656.
53. MacIntyre, F. On reconciling optical and acoustic bubble spectra in the mixed layer. In: Oceanic whitecaps and their role in air-sea exchange processes. Monanhan E C, O'Muircheartaigh, I, eds D Reidel Pub Co, Dordrecht, Holland, 1986; pp. 95-100.
54. Wolf, J. Investigation of bubbly flow by ultrasonic tomography. Part. Part. Syst. Charact. 1988; 5: 170-173.
55. Minnaert, M. On musical air-bubbles and sounds of running water, Phil. Mag. 1933; 16: 235-248.
56. Walton, A J, Reynolds, G T. Sonoluminescence. Advances in Physics 1984; 33: 595-660.
57. Strasberg, M. Gas bubbles as sources of sound in liquids. J Acoust Soc Am 1956; 28: 20-26.
58. Fitzpatrick H M, Strasberg, M. Hydrodynamic sources of sound. In: Proc 1st Symp on Naval hydrodynamics, Washington DC, NAS-NRC Publ 515 pp241-280. Washington: US Printing Office 1957.
59. Leighton, T G and Walton, A J. An experimental study of the sound emitted from gas bubbles in a liquid. Eur J Phys 1987; 8: 98-104.
60. Longuet-Higgins M S, Kerman, B R, Lunde K. The release of air bubbles from an underwater nozzle. J Fluid Mech 1991; 230: 365-390.
61. Leighton T G, Schneider, M F and White, P R. Study of bubble fragmentation using optical and acoustic techniques. Proc 3rd Conf on Sea Surface Sound (Scripps Inst. Ocean., San Diego 1994). Accepted for publication.
62. Pumphrey, H C, Crum, L A, Bjørnø, L. Underwater sound produced by individual drop impacts and rainfall. J Acoust Soc Am 1989; 85: 1518-1526.
63. Pumphrey, H C, Elmore P A. The entrainment of bubbles by drop impacts. J Fluid Mech 1990; 220: 539-567.
64. Medwin, H, Kurgan, A, Nystuen, J A. Impact and bubble sound from raindrops at normal and oblique incidence. J Acoust Soc Am 1990; 88: 413-418.
65. Pumphrey, H C, Walton A J. Experimental study of the sound emitted by water drops impacting on a water surface. Eur J Phys 1988; 9: 225-231.
66. Medwin, H, Beaky, M W. Bubble sources of the Knudsen sea noise spectra. J Acoust Soc Am 1989; 86: 1124-1130.
67. Updegraff, G E, Anderson, V C. Bubble noise and wavelet spills recorded 1m below the ocean surface. J Acoust Soc Am 1991; 89: 2264.
68. Nishi, R Y. Ultrasonic detection of bubbles with Doppler flow transducers. Ultrasonics 1972 10: 173-179.
69. Medwin H. Counting bubbles acoustically: a review. Ultrasonics 1977; 15: 7-14.
70. Thorpe, S A, Hall, A J. The characteristics of breaking waves, bubble clouds and near-surface currents observed using side-scan sonar. Continental Shelf Res 1983; 1: 353-384.
71. Farmer, D M, Vagle, S. Waveguide propagation of ambient sound in the ocean-surface bubble layer. J Acoust Soc Am 1989; 86: 1897-1908.
72. Daniels, S, Paton, W D M, Smith, E B. An ultrasonic imaging system for the study of decompression induced gas bubbles. Undersea Biomed. Res., 1979; 6: 197.
73. Mackay, R S, Rubisson, J R. Decompression studies using ultrasonic imaging of bubbles. IEEE Trans on Biomed Eng 1978; BME-25: 537-544.
74. Fry, F J, Goss, S A. Further studies of the transkull transmission of an intense focused ultrasonic beam: lesion production at 500kHz. Ultrasound Med biol 1980; 6; 33-38.
75. Frizzel, L A, Lee, C S, Aschenbach, P D, Borrelli, M J, Morimoto, R S, Dunn, F. Involvement of ultrasonically induced cavitation in hind limb paralysis of the mouse neonate. J Acoust Soc Am 1983; 74: 1062-1065.
76. Watmough, D J, Davies, H M, Quan, K M, Wytch, R, Williams, A R. Imaging microbubbles and tissues using a linear focussed scanner operating at 20MHz: possible implications for the detection of cavitation thresholds. Ultrasonics 1991; 29: 312.
77. ter Haar, G R, Daniels, S. Evidence for ultrasonically induced cavitation *in vivo*. Phys Med Biol 1981; 26: 1145-1149
78. Morton, K I, ter Haar, G R, Stratford, I J, Hill, C R. The role of cavitation in the interaction of ultrasound with V79 Chinese hamster cells *in vitro*. Br J Cancer 1982; 45: Suppl. V. 147.
79. ter Haar, G R, Daniels, S, Morton, K. Evidence for acoustic cavitation *in vivo*: Thresholds for bubble formation with 0.75MHz continuous-wave and pulsed beams. IEE Trans. UFFC 1986; 33: 162-164.
80. Beck, T W, Daniels, D, Paton, W D M, Smith, E B. The detection of bubbles in decompres-

sion sickness. Nature 1978; 276: 173.
81. Fowlkes, J B, Carson, P L, Chiang, E H, Rubin, J M. Acoustic generation of bubbles in excised canine urinary bladders. J Acoust Soc Am 1991; 89: 2740-2744.
82. Bleeker, H J, Shung, K K, Barnhart, J L. Ultrasonic characterization of Albunex, a new contrast agent. J Acoust Soc Am 1990; 87: 1792-1797.
83. Fairbank, W M, Scully, M O. A new non-invasive technique for cardiac pressure measurement: resonant scattering of ultrasound from bubble. IEEE Trans on Biomed Eng 1977; BME-24: 107-110.
84. Commander, K W, Moritz, E. Off-resonance contribution to acoustical bubble spectra. J Acoust Soc Am 1989; 85: 2665-2669.
85. Commander, K W, McDonald, R J. Finite-element solution of the inverse problem in bubble swarm acoustics. J Acoust soc am 1991; 89: 592-597.
86. Clay, C S, Medwin, H. Acoustical Oceanography: Principles and Applications. 1977 Wiley, New York.
87. Medwin, H, Breitz, N D. Ambient and transient bubble spectral densities in quiescent seas and under spilling breakers. J Geophys Res 1989; 94: 12751-12759.
88. Breitz, N, Medwin, H. Instrumentation for in situ acoustical measurements of bubble spectra under breaking waves. J Acoust Soc Am 1989; 86: 739-743.
89. Fanelli, M, Prosperetti, A, Reali, M. Shape oscillations of gas-vapour bubbles in liquids. Part 1: Mathematical formulation. Acustica 1984; 55: 213-223.
90. Donskoi, D M, Zamolin, S V, Kustov, L M, Sutin, A M, Nonlinear backscattering of acoustic waves in a bubble layer. Acoustic Letters 1984; 7: 131.
91. Butkovsky, O, Ya, Zabolotskaya, E A, Kravtsov, Yu A, Petnikov, V G, Ryabikin, V V. Possibilities of active nonlinear spectroscopy of inhomogeneous condensed media. acta physica slovaca 1986; 36:58.
92. Tucker, D G, Wesby, V G. Ultrasonic monitoring of decompression. Lancet 1968; 1: 1253.
93. Miller, D L. Ultrasonic detection of resonant cavitation bubbles in a flow tube by their second harmonic emissions. Ultrasonics 1981; 19; 217-224.
94. Miller, D L, Williams, A R, Gross, D R. Characterisation of cavitation in a flow-through exposure chamber by means of a resonant bubble detector. Ultrasonics 1984; 22: 224-230.
95. Vacher, M, Giminez, G, Gouette, R. Nonlinear behaviour of microbubbles: application to their ultrasonic detection. Acustica 1984; 54: 274-283.
96. Blackstock, D T. History of nonlinear acoustics and a survey of Burgers' and related equations. In: Nonlinear Acoustics, Proceedings of the Symposium held at Applied Research Laboratories, The University of Texas at Austin, 1969, ed. Muir T G (AD 719 936), pp. 1-27.
97. Pfeiler, M, Matura, E, Iffländer, H, Seyler, G. Lithotripsy of renal and biliary calculi: physics, technology and medical-technical application. Electromedica 1989; 57: 52-63.
98. Newhouse, V L, Shankar, P M. Bubble size measurement using the nonlinear mixing of two frequencies. J Acoust Soc Am, 1984; 75: 1473-1477.
99. Chapelon, J Y, Shankar, P M, Newhouse, V L. Ultrasonic measurement of bubble cloud size profile. J Acoust Soc Am 1985; 78: 196-201.
100. Schmitt, R M, Schmitt, H J, Siegert, J. *In vitro* estimation of bubble diameter distribution with ultrasound. IEEE Eng in Med and Biol Soc 1987; 9th Ann Conf, 13-6.
101. Siegert, J, Schmitt, R M, Schmitt, H J, Fritzsch, T. Application of a resonance method for measuring the size of bubbles in an echocontrast agent. IEEE Eng in Med and Biol Soc 1987; 9th Ann Conf, 13-6.
102. Quain, R M, Waag, R C, Miller, M W. The use of frequency mixing to distinguish size distributions of gas-filled micropores. Ultrasound Med Biol 1991; 17: 71-79.
103. Miller, D L. Experimental investigation of the response of gas-filled micropores to ultrasound. J Acoust Soc Am 1982; 71: 471-476.
104. Miller, D L. Theoretical investigation of the response of gas-filled micropores and cavitation nuclei to ultrasound. J Acoust Soc Am 1983; 73: 1537-1544.
105. Miller, D L. On the oscillation mode of gas-filled micropores. J Acoust Soc Am 1985; 77(3): 946-953.
106. Chapelon, J Y, Newhouse, V L, Cathignol, D, Shankar, P M. Bubble detection and sizing with a double frequency Doppler system. Ultrasonics 1988; 26: 148-154.
107. Cathignol, D, Chapelon, J Y, Newhouse, V L, Shankar, P M. Bubble sizing with high spatial resolution. IEEE Trans. Ultrasonics, Ferroelectrics and freq. Control 1990; 37: 31.
108. Ostrovsky, L A, Sutin, A M. Nonlinear sound scattering from subsurface bubble layers. In: Natural physical sources of underwater sound. Kerman, B R, ed. Kluwer academic publishers (Dordrecht, The Netherlands), 1992.
109. Jordan, D W, Smith, P. Nonlinear ordinary differential equations. 2nd edition (1987), Oxford University Press, Chapter 7.
110. Leighton, T G, Lingard, R J, Walton, A J and Field, J E. Bubble sizing by the nonlinear scattering of two acoustic frequencies. In: Natural physical sources of underwater sound. Kerman, B R, ed. Kluwer academic publishers (Dordrecht, The Netherlands), 1992.
111. Leighton, T G, Lingard, R J, Walton, A J, Field, J E. Acoustic bubble sizing by the combination of subharmonic emissions with an imaging frequency. Ultrasonics 1991; 29: 319-323.
112. Phelps, A D and Leighton, T G. Investigations into the use of two frequency excitation to accurately determine bubble sizes. Proc. IUTAM Conf. on Bubble Dynamics and Interface Phenomena (Birmingham 1993). In press.
113. Phelps, A D and Leighton, T G. Automated bubble sizing using two frequency excitation techniques. Proc 3rd Conf on Sea Surface Sound (Scripps Inst. Ocean., San Diego 1994). In press.
114. Korman, M F, Beyer, R T. Nonlinear scattering of crossed ultrasonic beams in the presence of turbulence in water: I Experiment. J Acoust Soc Am 1988; 84: 339-349.
115. Korman, M F, Beyer, R T. Nonlinear scattering of crossed ultrasonic beams in the presence of turbulence in water: II Theory. J Acoust Soc Am 1989; 85: 611-620.
116. Bunkin, F V, Vlasov, D V, Zabolotskaya, E A, Kravstov, Yu, A. Active acoustic spectroscopy of bubbles. Sov Phys Acoust 1983; 29: 99-100.
117. Ostrovskii, L, Sutin, A. Nonlinear acoustic methods in diagnostics. In: Ultrasound diagnostics, Grechova ed, Gorky, pp. 139-150 (in Russian).
118. Sandler, B, Selivanovskii, D, Sokolov, A. Measurement of gas bubble concentration on the sea surface. Doklady Adademii Nauk SSSR. 260, 6, 1474-1476 (1981, in Russian).
119. Naugol'nykh, K A, Rybak, S A. Interaction of sound waves in scattering by bubbles. Sov Phys Acoust 1987; 33: 94.

IOCE 94

The 1994 International Offshore Contracting and Subsea Engineering exhibition and Conference organised by Spearhead Exhibitions, will be held at the Conference Centre, Aberdeen 4-6 October.

As well as addressing the more obvious cost control initiatives, the IOCE 94 conference will address some of these new approaches:- standardisation - the advantage and disadvantages; achieving a balance between safety and cost reduction and risk assessment; new subsea production/floating production options; more effective partnering/ contracting strategies. The range of products and services on display at the related exhibition from 100+ international companies will reflect the very latest enabling technologies and operational practice to allow the industry to maximise the profitability of existing developments and new frontier areas.

Among the exhibitors will be

TECHNICAL SOFTWARE CONSULTANTS LTD. will show inspection systems for both underwater and topside use. Their most newsworthy exhibit will be the control system for an ROV mounted robotic arm. This is the culmination of work done by Mobil, Slingsby Engineering, TSC and University College London. The topside ACFM instrument will be their most photogenic exhibit. Tel M Boyden on 0908 220255.

THORN COMMUNICATIONS AND TELECONTROL SYSTEMS will show their autonomous control buoy and wave height sensor. The autonomous control buoy is their most newsworthy exhibit - it is supported by a European Union Thermie grant and has recently been deployed to sea. A large, detailed model of the autonomous control buoy will be on show. Tel Dr M Jackson on 0932 743133.

AMITEC LTD will show flexible pipe monitoring and inspection systems; ROV ultrasonic wall thickness mapping; and bolt inspection. Their most newsworthy exhibit will be flexible pipe inspection and polymer ageing monitoring - a unique technology. Tel Margaret Watson on 0224 898 282.

AEA will show new releases of their software products PLAC and CFOS-FLOW30 in addition to their erosion, corrosion and pipe integrity capabilities. Tel Gavin Butcher on 0235 436748.

ALAN COBHAM ENGINEERING who will show liquid and gaseous hydrocarbon conditioning equipment/systems and fuel gas heaters and will be publicising new gas condensate clean-up techniques. Tel Jill Murphy on 0258 451 441.

TRITECH INTERNATIONAL LTD. will show their SCU-3 multitasking survey processor and associated survey sensors; manipulators and dredging systems. Their most newsworthy exhibit will be the compact, powerful and cost effective SCU-3 multitasking processor which simultaneously controls and displays multiple sensors in real-time. Tel Kevin Parker on 0224 744111.

TWI will graphically portray their support services for the engineering industry worldwide. They come to the show soon after the official opening of their newly commissioned £300,000+ 6.5m dive tank and underwater operations at TWI-North in Middlesbrough; the centre has been developed for underwater training, examinations, testing and equipment and process development. Internal press contact: Tel Rod Griggs on 0223 891162.

EUROPEAN UNION - the Directorate-General for Energy of the European Commission will be promoting its THERMIE programme, which plays a major role in the European Union's energy strategy. Innovative, near-market, oil and gas technologies developed within the EU member states will be demonstrated by five participating companies - AEA Technology, UK; Alfapi SA, Greece; Mors Environment, Francel; Seatec BV, The Netherlands; WD Loth & Co Ltd, UK. Tel J Kennedy on +32 2 295 1111